Journal of Luminescence 289 (2026) 121643

Contents lists available at ScienceDirect

Journal of Luminescence

journal homepage: www.elsevier.com/locate/jlumin

Full Length Article

Unlocking simultaneous blue and green phosphorescence from three-donors-single acceptor conjugate

Harshini Dhara [a,1], Manoj Upadhyay [a,1], Manjeet Singh [a], Raktim Deka [a], Tanika Sharma [a], Sreerang Peethambaran [a], Michał Andrzej Kochman [b,c], Christof Hättig [b], Debdas Ray [a,*]

[a] Advanced Photofunctional Materials Laboratory, Department of Chemistry, Shiv Nadar University, Delhi NCR, Gautam Buddha Nagar, Uttar Pradesh, 201314, India
[b] Lehrstuhl für Theoretische Chemie, Ruhr-Universität Bochum, D-44780, Bochum, Germany
[c] Institute of Physical Chemistry of the Polish Academy of Sciences, Ul. Marcina Kasprzaka 44/52, 01-224, Warsaw, Poland

ARTICLE INFO

Keywords:
Multiple-donors-acceptor
Absorption
Energy
Phosphorescence
Quantum mechanics

ABSTRACT

Achieving dual room-temperature phosphorescence (DRTP) in twisted organic systems is rare. We explored how a benzophenone host triggers simultaneous blue and green RTP in a three-donor-single-acceptor molecule (Cz3Q). Spectroscopy and quantum calculations reveal that Cz3Q holds a wide singlet–triplet gap (~0.4 eV), which blocks delayed fluorescence despite a clear separation of frontier orbitals. Instead, DRTP emerges from Dexter-type triplet transfer, where the host channels energy to both donor and acceptor regions of Cz3Q because the triplet states of host and guest align closely in energy. As a result, Cz3Q bypasses delayed fluorescence yet achieves simultaneous dual phosphorescence. This insight shows how a precise host–guest blend can unlock new emission pathways in organic systems. By guiding energy through balanced triplet levels, we demonstrate a data security application with remarkable efficiency and color versatility.

1. Introduction

Room-temperature phosphorescence (RTP) offers immense potential for sensors [1–6], bioimaging [7–12], and data security [13–19] because it involves long-lived triplet energy [20,21]. However, designing organic materials to emit phosphorescence remains challenging. The key challenge is that phosphorescence from the triplet states is spin-forbidden, and therefore relatively inefficient. Population transfer from the singlet states into the triplet states through intersystem crossing (ISC) is also slow. In the past, researchers have used heavy metal complexes to boost spin-orbit coupling (SOC) and improve phosphorescence [22]. However, it accompanied high costs and harsh production methods. Organic RTP materials offer a better alternative as they are cheaper, easier to process, and more flexible in structure. Yet, there are trade-offs: weak SOC, sensitivity to oxygen, and energy loss through non-radiative decay [22]. To improve RTP in organics, researchers have developed several methodologies, such as atoms with lone electron pairs [22,23], heavy atoms to boost SOC effects [22,24–27], aggregation [14,17,28–30], and followed principles like El-Sayed's rules [31] and the energy gap law [14,15]. Structural strategies include the use of photo-switches [32], twisted donor-acceptor [1,33–35], donor-linker-acceptor [15,36–40], single crystals [33], polymers [41,42], and metal-organic frameworks [43] to help stabilize the excited states and reduce energy loss. Despite these great achievements, achieving dual RTP (DRTP), where two triplet states emit light, is even tougher because it defies Kasha's rule, which limits emission to the lowest excited state. DRTP can occur in two ways: if the gap between T_1 and T_2 is wide enough to slow internal conversion, or if that gap is small and allows thermal population from T_1 to T_2 [16,44–50]. Another promising method is triplet-to-triplet energy transfer (TTET) [44–48,51–57], which swaps energy and spin between nearby molecules or two parts of the same molecule, ideally within 10 Å. TTET shows promise, but the design principles for DRTP systems, especially those using TTET, are not yet fully understood.

Here, we designed **Cz3Q**, a twisted multiple donor-single acceptor molecule and blended it with benzophenone (BP) (Fig. 1). This combination aligned energy levels and triggered TTET. On its own, **Cz3Q** only fluoresces. However, when mixed with BP, it showed clear DRTP. These findings prove that TTET can trigger long-lasting blue and green RTP in twisted organic materials, opening a path toward data security

* Corresponding author.
E-mail address: debdas.ray@snu.edu.in (D. Ray).
[1] Share equal authorship.

https://doi.org/10.1016/j.jlumin.2025.121643
Received 4 September 2025; Received in revised form 17 October 2025; Accepted 1 November 2025
Available online 2 November 2025
0022-2313/© 2025 Elsevier B.V. All rights are reserved, including those for text and data mining, AI training, and similar technologies.

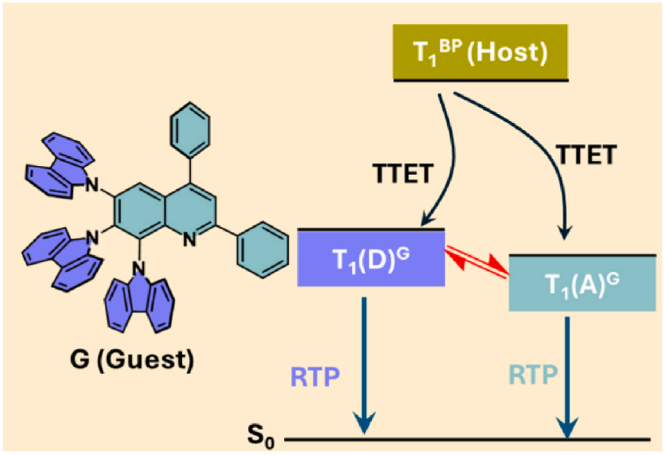


Fig. 1. Molecular design with dual phosphorescence.

applications.

2. Experimental and theoretical procedure

2.1. Chemicals and materials

All reagents and deuterated solvents were obtained from commercial sources and used without further purification unless otherwise mentioned. 1,2,3-trifluoro-4-nitrobenzene, aniline, phenylacetylene, benzaldehyde, 2-phenylnitrobenzene, triphenylphosphine, K^{t}OBu, and the host matrix (Benzophenone) were purchased from Sigma–Aldrich. Ethyl acetate, hexane, Na_2SO_4, NaOH, and stannous chloride were purchased from local sources. Dimethyl formamide (DMF) was dried and distilled over calcium hydride. Spectroscopic grade solvents were used for all spectroscopic measurements.

2.2. Synthesis

Cz3Q was synthesized by reacting 2,3,4-tri(9H-carbazol-9-yl)aniline, benzaldehyde, and 1-ethylbenzene, in nitromethane at 80 °C in the presence of a catalytic amount of molecular iodine under oxygenated conditions (Scheme 1) [24,33,34,58–60]. Similarly, compound **QPP** (2, 4-diphenylquinoline) was synthesized using the above procedure except using aniline separately. All the compounds were characterized by NMR spectroscopy, high-resolution mass spectrometry, SCXRD, and HPLC analysis of the vacuum sublimated samples (Supporting Information).

2.3. Characterization of sample

2.3.1. X-ray diffraction methods

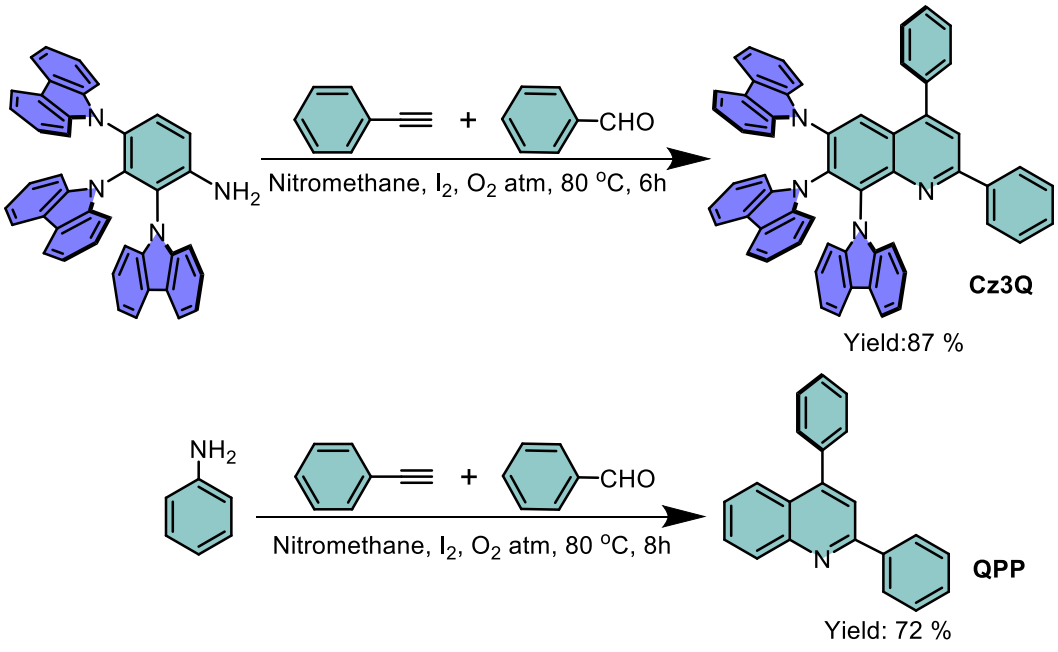
We collected single-crystal X-ray diffraction data using a D8 Venture 1 μS microfocus dual-source Bruker APEX3 diffractometer. It includes an Oxford cryogenic system and a PHOTON 100 CMOS detector. At room temperature, we mounted single crystals on glass fiber tips. All the data was collected and processed at room temperature using APEX2 [61] for acquisition, SAINT for cell refinement and data reduction, and SHELXT [62] to solve the structure. We refined the structure with SHELXL2014. Molecular graphics were created using Ortep-3 [63] on a Windows system. The process followed standard crystallographic methods from Bruker and Sheldrick software tools.

2.3.2. Photophysical property measurement

We measured steady-state absorbance using a Cary 8454 UV/Vis instrument from Agilent. A HORIBA Fluorolog-3 spectrofluorometer with an integrating sphere recorded the emission and quantum yield. We used a JANIS cryostat to carry out temperature-dependent PL measurements. All spectra were reference corrected to account for variations in both the excitation source and the detector response. For absolute quantum yield measurements in solid-state, we used a HORIBA Quanta-Phi 6 integrating sphere. We performed HPLC analysis on a Waters Alliance system with an e2695 separation module and a 2998 photodiode-array detector. Each step followed reliable, consistent methods for accurate data collection [24,33,58].

2.3.3. Measurement of lifetime

We performed lifetime analysis using a HORIBA Fluorolog-3 spectrofluorometer with pulsed nano-LEDs at 390 nm and spectral-LEDs at 400 nm. Phosphorescence measurements used a pulsed xenon lamp and gating electronics to control the timing and width of the detection



Scheme 1. Synthesis Scheme of Cz3Q and QPP.

window. We applied a 50-μs delay to capture phosphorescence spectra for all samples. For phosphorescence lifetime analysis, we set the excitation source delay to 1 % relative to the sample window. Full details of the method are available in the published literature for reference. [24, 33,58].

3. Result and discussion

3.1. Single crystal X-ray diffraction analysis

We grew crystals of **Cz3Q** using a binary solvent mixture of toluene and hexane at RT. Single crystal X-ray diffraction (SCXRD) confirmed a twisted structure in **Cz3Q**. The carbazole groups covalently bonded to the C6, C7, and C8 positions of the 2,4-diphenylquinolinyl acceptor via three C−N single bonds show a clear deviation from planarity (Fig. 2a, Fig. S6). Torsion angles are −57.04°, −66.93°, and −59.24° along the C00G– N4–C8–C9, C8–C7–N3–C47, and C5–C6–N2–C23 atoms, respectively (Fig. 2b–Table S1). These values reflect a consistent angular twist between donor and acceptor units. The SCXRD data also shows that the carbazole (donor) and 2,4-diphenylquinolinyl (acceptor) groups align in an angular orientation. The skewed Cz orientations with respect to the acceptor aligns with electrochemical experiments, suggesting a decoupling between the donor and acceptor (Fig. S7, Table S3). We expect that this angular geometry controls the charge transfer (CT) state by separating the highest occupied (HOMO) and lowest unoccupied (LUMO) molecular orbitals [24,33,58]. The distinct spatial arrangement of these orbitals likely plays a key role in tuning the electronic behaviour. Furthermore, TGA confirmed high thermal stability, with only 5 % weight loss occurring at 376.8 °C, highlighting the compound's durability and potential for optoelectronic applications (Fig. S8).

3.2. Quantum chemistry analysis

We used DFT/TDDFT geometry optimizations at the LC-wPBE/def2-SVP (w = 0.175) level of theory [65] (TURBOMOLE 7.6 [64]) followed by ADC(2)/def2-SVP single-point calculations to investigate the electronic properties of Cz3Q [66,67]. The HOMO is mostly contributed by the Cz-7/Cz-8 donors along with fewer contribution by the fused benzene ring of the quinoline part. While the 2,4-diphenylquinolinyl acceptor and small contribution from the N atoms of the donors are seen to construct the LUMO, suggesting minimum overlap between HOMO/LUMO conducive for CT (Fig. S9). Natural transition orbital (NTO) analysis shows that the S_1 state of **Cz3Q** displays a distinct CT character, as the occupied and virtual NTOs are localized on the donor (mainly Cz-8 and minor contribution from the fused-phenyl ring of the quinoline segment, and the N atom of Cz-7) and acceptor (predominant) components, respectively (Fig. 3). For the T_1 state, the occupied and virtual NTOs are both majorly located on the acceptor group, revealing a locally excited state (^{3}LE). Additionally, the theoretical singlet-triplet gap (ΔE_{ST}), was found to be ~0.4 eV, which is too high for TADF to occur in the guest, pointing to only radiative decay in the form of fluorescence from the S_1^{CT} state (Fig. 3). The vertical transition energy from S_1 to S_0 was found to be 2.50 eV (~495 nm) which closely matches with the experimental fluorescence spectra recorded in toluene solution (Fig. 4, Fig. S9).

3.3. Absorption characteristics in solutions

Ultraviolet–visible absorption studies of **Cz3Q** solutions show peaks around 320–330 nm and 370–430 nm (Fig. 4a). As solvent polarity increases, the lower-energy peak shifts to shorter wavelengths, consistent with the previous report [33]. This shift confirms a CT character in the absorption band (Fig. S11). The higher-energy band remains insensitive to solvent polarity, suggesting it results from a local π−π* transition. This band, found between 300 and 350 nm, aligns with the absorption profiles of the donor and acceptor parts (Fig. 4b). The new lower-energy band appears only when both parts combine, indicating that D-A coupling in the ground state drives this CT absorption.

3.4. Emission characteristics in solution and solid state

Cz3Q shows strong CT (S_1^{CT}) in its excited state (λ_{ex} = 400 nm), confirmed by solvent-dependent steady-state emission measurement (Fig. 4c; Fig. S12). In toluene, the emission shows a nanosecond lifetime of 10.86 ns (λ_{ex} = 400 nm, PLQY = ~35 %) (Fig. S14, Table S4). To test thermally activated delayed fluorescence (TADF) [33], we measured emission and lifetimes at room temperature under ambient, and argon conditions (Fig. 4d; Table S5). The lifetimes stayed almost consistent, with 7.86 ns in air and 9.78 ns in argon, showing no signs of triplet involvement. This confirms that only the S_1^{CT} emits under these conditions. We recorded phosphorescence at 77 K (λ_{ex} = 400 nm, 0.2 ms delay) (Fig. S15a). The spectrum revealed a vibrational structure from a triplet local excited state (^{3}LE) around 530–570 nm. Notably, this emission is red shifted by 20 nm compared to the phosphorescence peak (T_1^A) of the acceptor **QPP** (Fig. S15b). This shift likely results from the altered triplet state of the acceptor when linked to three donor units in **Cz3Q**. The calculated ΔE_{ST} is ~0.40 eV, which matches the theoretical ΔE_{ST} (Figs. S9 and 15a), and is too high for TADF in **Cz3Q**. Similar results appeared in a thin film blended with 1 wt% of 1,3-bis(N-Carbazolyl)benzene (mCP) (Fig. S16).

3.5. Emission characteristics of Host–Guest binary systems

Cz3Q was blended with benzophenone (BP) using a 1:1000 M ratio through melt-casting (Supporting Information). This melt-casted blend was then studied for its photophysical properties. Upon excitation at

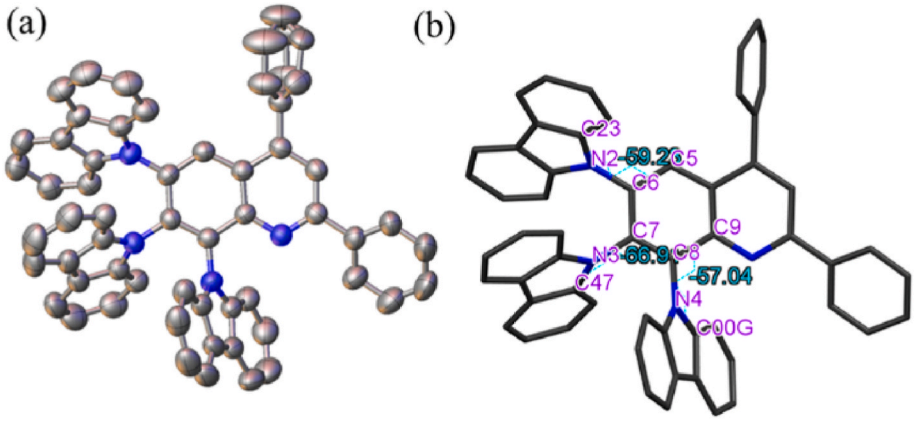


Fig. 2. (a) Oak Ridge thermal ellipsoid plots (50 % probability ellipsoids) and (b) selected torsions of Cz3Q. H atoms are removed for the sake of clarity.

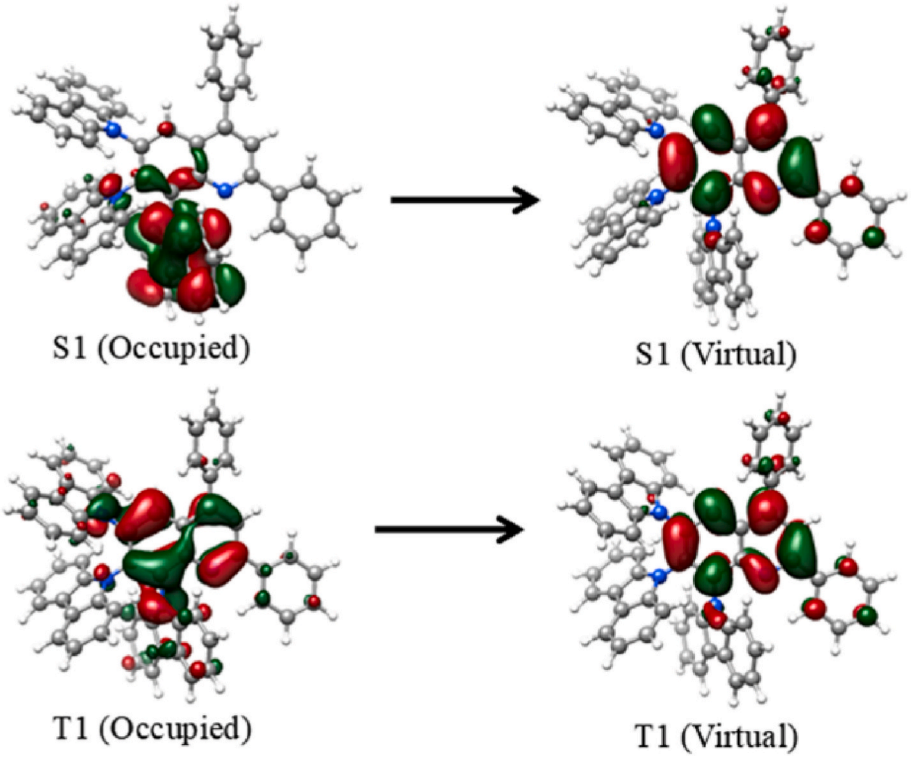


Fig. 3. Occupied and virtual natural transition orbitals of S_1 and T_1 states calculated at ADC(2)/def2-SVP level of theory.

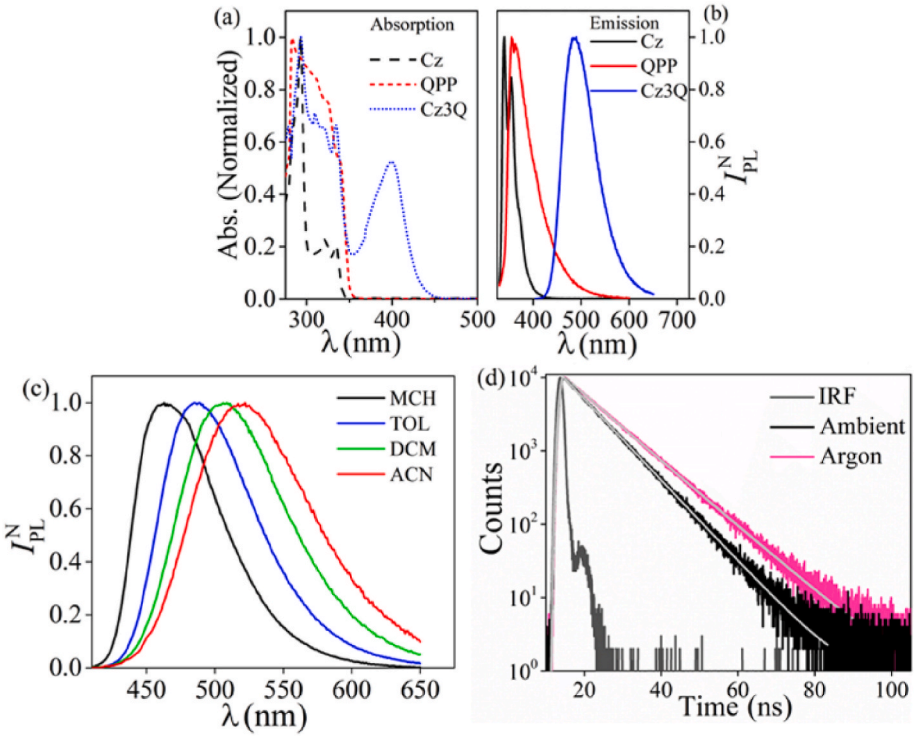


Fig. 4. Comparison of (a) absorption and (b) emission spectra of donor, acceptor and Cz3Q (10 μM) in toluene (λ_{ex} = 320 nm) under ambient conditions. (c) Steady-state PL in different solvents. (d) Lifetime decays of Cz3Q at room-temperature under argon and ambient conditions (λ_{ex} = 400 nm) in toluene.

370 nm under ambient conditions, the blend emitted light peaking at 490 nm, with a broad tail from 550 to 620 nm (PLQY = 45 %) (Fig. 5a). The excitation spectra match the absorption spectra, and the emission profile remained consistent, confirming the absence of heterogeneity in both ground and excited states (Fig. S17). The 490 nm peak corresponds to fluorescence from S_1^{CT}, confirmed by a fluorescence lifetime of 13.35 ns (Fig. 5b). Phosphorescence measurements (0.05 ms detector delay) revealed two emission regions; one narrow band appeared between 495

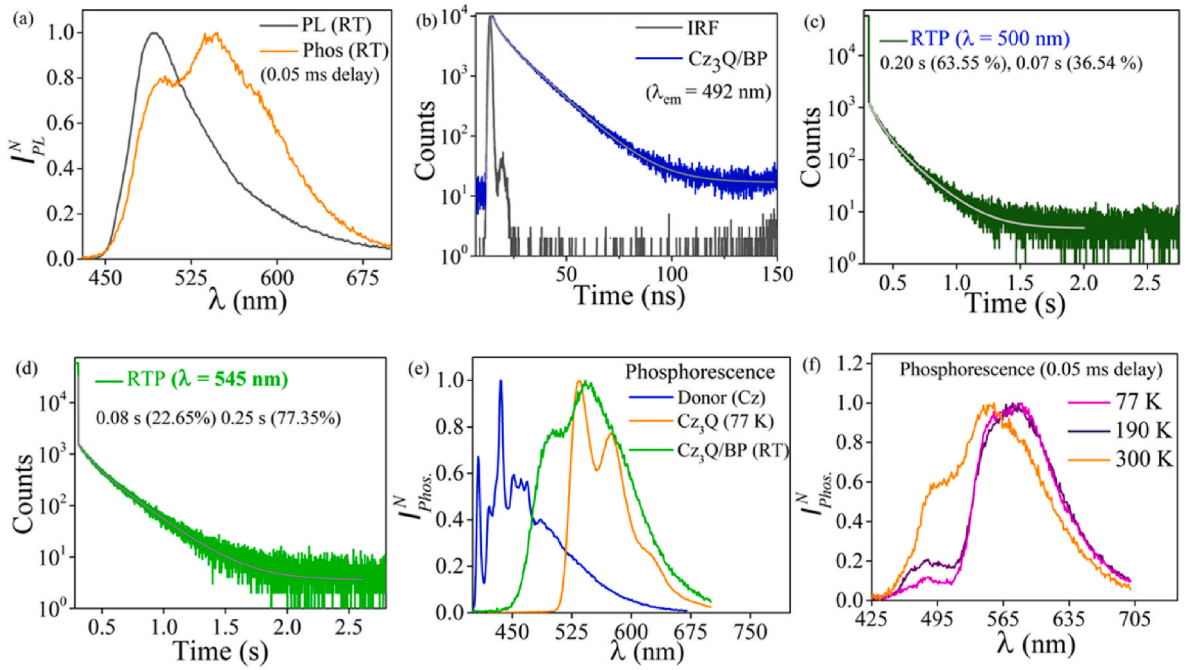


Fig. 5. (a) Steady-state photoluminescence (PL) and phosphorescence spectra of the Cz3Q:BP blend (1:1000 M ratio) under ambient conditions. (b) Fluorescence lifetime profile and (c, d) phosphorescence lifetime profiles of the dual-room-temperature phosphorescence (DRTP) feature (λ_{ex} = 370 nm). (e) Comparison of phosphorescence spectra for the donor at 77K, Cz3Q at 77K, and Cz_3Q:BP blend at RT. (f) Temperature-dependent phosphorescence spectra of the Cz3Q:BP (1:1000 M ratio) blend.

and 505 nm, and a broader range extended from 515 to 620 nm akin to the steady state PL spectrum. Phosphorescence decay at RT confirmed long-lived emission (500 nm: $\tau_1 = 0.2$ ms and $\tau_2 = 70.7$ ms; 545 nm: $\tau_1 = 0.3$ ms, $\tau_2 = 81.4$ ms; $\lambda_{ex} = 370$ nm) associated with the DRTP feature (Fig. 5c and d). Comparing the phosphorescence spectra of the donor (Cz), acceptor, the D-A conjugate, and the sensitizer showed that the higher energy band (T_2) results from the donor's triplet state (T_1^D), while the lower energy broadband (T_1) arises from a modified triplet state of the acceptor, i.e., T_1^A of **Cz3Q** (Fig. 5e, Fig. S18). When tested across temperatures ranging from 77 K to 330 K under vacuum, the high-energy emission band stayed consistent except for an increase in intensity (Fig. 5f). The lower-energy emission band shifted slightly, reinforcing the presence of DRTP via thermal population of T_2 (T_1^D) from T_1(T_1^A), consistent with the literature [46,47]. Energy gaps calculated from the steady-state and phosphorescence spectra revealed the following values: $\Delta E_{S1^{CT}-T1^{BP}}$ was small (0.16 eV), enabling efficient ISC from S_1^{CT} to T_1^{BP} (Fig. S18, Table S7). Other key energy gaps were 0.04 eV (T_1^{BP}–T_1^D), 0.27 eV (T_1^{BP}–T_1^A), and 0.23 eV (T_1^D–T_1^A), which supported energy transfer between closely aligned triplet states. These findings show that BP's higher-energy triplet state (T_1^{BP}) acts as a sensitizer, transferring energy to lower-energy states in **Cz3Q** through multiple Dexter-type triplet–triplet energy transfer (TTET) pathways (Figs. 1 and 6a). This mechanism explains the observed DRTP with a persistent emission feature. The observed room-temperature phosphorescence (RTP) behavior can be rationalized through a triplet–triplet energy transfer (TTET) mechanism facilitated by benzophenone. The presence of multiple donor units appears to modulate the triplet energy landscape of the system, subtly lowering or shifting the triplet energy of the donor–acceptor ensemble. This modification increases the energy gap between the triplet states participating in TTET, thereby reducing the rate of energy transfer. The slower TTET process prolongs the excited triplet-state lifetime, which directly enhances phosphorescence persistence and intensity. Experimental evidence, particularly the observed extended afterglow and prolonged decay profiles, substantiates this interpretation. These findings align closely with previously reported studies, which describe analogous triplet–triplet energy transfer and

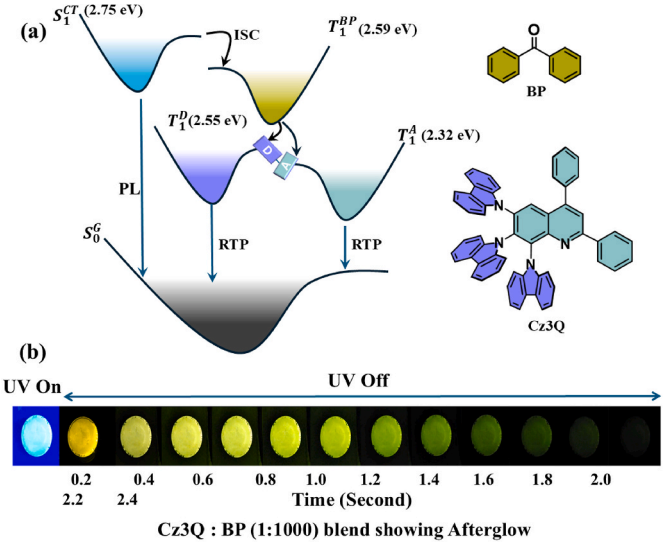


Fig. 6. (a) Energy diagram for host-sensitized dual RTP under ambient conditions. (b) Data security application pattern of "O" under illumination with a 365 nm lamp using the Cz3Q:BP (1:1000) blend.

phosphorescence behaviors under comparable conditions [16,48, 51–55]. Thus, benzophenone serves a critical role in enabling efficient intermolecular TTET at room temperature, a process unattainable in a single-component systems, leading to pronounced blue and green RTP emissions within the host–guest framework.

3.5.1. *Data security applications*

Fig. 6b shows the persistent RTP features of blend samples with1:1000 M ratio. Using the longer lifetime of the BP:Cz3Q blend, we demonstrated its potential for encryption and decryption, as shown in Fig. 6b. Under 365 nm light, the "O" pattern made from BP:Cz3Q

became blue-white due to the combined fluorescence and phosphorescence of the emitter. When the light was switched off, only the phosphorescence emission as golden to green afterglow "O" pattern remained. This afterglow, caused by the blend, stayed visible to the naked eye for a period of ~2.4 s (web enhanced object).

4. Conclusions

In summary, we successfully achieved simultaneous blue and green room-temperature phosphorescence in a purely organic system by blending a three-donor–one-acceptor molecule (Cz3Q) with benzophenone (BP) as the host matrix. Spectroscopic studies and quantum chemical calculations revealed that Cz3Q possesses a large singlet–triplet energy gap (~0.4 eV), which suppresses delayed fluorescence. However, when combined with BP, efficient Dexter-type triplet–triplet energy transfer (TTET) occurs due to the close alignment of triplet energy levels between BP and Cz3Q. This TTET pathway channels energy to both the donor and acceptor sites of Cz3Q, enabling persistent dual phosphorescence at room temperature. The study establishes a clear mechanistic link between host–guest energy alignment and dual triplet emission, demonstrating that a judiciously chosen host can unlock new radiative pathways in twisted donor–acceptor architectures. Furthermore, the long-lived afterglow of the BP:Cz3Q blend enables data encryption and decryption, showcasing its potential in data security and anti-counterfeiting applications. Overall, this work highlights how subject–object physical engineering, through precise energy-level matching in host–guest systems, can serve as a versatile design strategy for developing next-generation multicolour organic phosphorescent materials and functional optoelectronic devices.

CRediT authorship contribution statement

Harshini Dhara: Validation, Investigation, Formal analysis, Data curation. **Manoj Upadhyay:** Validation, Investigation, Formal analysis, Data curation. **Manjeet Singh:** Validation, Formal analysis. **Raktim Deka:** Validation, Formal analysis. **Tanika Sharma:** Validation, Formal analysis. **Sreerang Peethambaran:** Validation, Formal analysis. **Michał Andrzej Kochman:** Validation, Formal analysis. **Christof Hättig:** Validation, Formal analysis. **Debdas Ray:** Writing – review & editing, Writing – original draft, Validation, Supervision, Software, Project administration, Methodology, Investigation, Funding acquisition, Formal analysis, Data curation, Conceptualization.

Declaration of generative AI and AI-assisted technologies in the manuscript preparation process

During the preparation of this work the author used [CHATGPT 5.0] in order to [improve writing language]. After using this tool, the author reviewed and edited the content as needed and takes full responsibility for the content of the published article.

Declaration of competing interest

The authors declare that they have no known competing financial interests or personal relationships that could have appeared to influence the work reported in this paper.

Acknowledgement

D. R. is grateful to the Science & Engineering Research Board (SERB) (CRG/2022/000128), Department of Science and Technology (DST), India, the Anusandhan National Research Foundation (ANRF) (ANRF/IRG/2024/000038/CS), India. H. D. thanks SNIoE for OUR grant and is grateful to the Deutscher Akademischer Austauschdienst (DAAD, German Academic Exchange Service) for the WISE Scholarship 2024 which allowed her to perform the quantum chemical calculations at Ruhr-Universität Bochum. M. U., M. S., S. P. and R.D. thank SNIoE for the fellowship.

Appendix A. Supplementary data

Supplementary data to this article can be found online at https://doi.org/10.1016/j.jlumin.2025.121643.

Data availability

Data will be made available on request.

References

[1] I. Bhattacharjee, N. Acharya, S. Karmakar, D. Ray, J. Phys. Chem. C 122 (2018) 21589–21597.
[2] T.Z. Sodia, K.E. Frank, A.A. Mendonsa, J.M. Branning Jr., K.J. Cash, ACS Sens. 10 (2025) 4873–4881.
[3] R. Tian, S. Gao, K. Li, C. Lu, Nat. Commun. 14 (2023) 4720.
[4] H. Ju, H. Zhang, L.X. Hou, M. Zuo, M. Du, F. Huang, Q. Zheng, Z.L. Wu, J. Am. Chem. Soc. 145 (2023) 3763–3773.
[5] E. Hamzehpoor, C. Ruchlin, Y. Tao, C.-H. Liu, H.M. Titi, D.F. Perepichka, Nat. Chem. 15 (2023) 83–90.
[6] J. Yu, H. Ma, W. Huang, Z. Liang, K. Zhou, A. Lv, X.-G. Li, Z. He, J. Am. Chem. Soc. Au 1 (2021) 1694–1699.
[7] J. Li, N. Niu, D. Wang, J. Zhu, X. Li, Q. Kong, B. Zhong Tang, D. Wang, Angew. Chem. Int. Ed. 64 (2025) e202413219.
[8] Y. You, Current opin, Chem. Biol. 17 (2013) 699–707.
[9] L. Zhang, J. Li, Y. Zhang, W. Dai, Y. Zhang, X. Gao, M. Liu, H. Wu, X. Huang, Y. Lei, Nat. Commun. 16 (2025) 3970.
[10] D. Li, Z. Liu, M. Fang, J. Yang, B.Z. Tang, Z. Li, ACS Nano 17 (2023) 12895–12902.
[11] F. Xiao, H. Gao, Y. Lei, W. Dai, M. Liu, X. Zheng, Z. Cai, X. Huang, H. Wu, D. Ding, Nat. Commun. 13 (2022) 186.
[12] H.-J. Yu, Q. Zhou, X. Dai, F.-F. Shen, Y.-M. Zhang, X. Xu, Y. Liu, J. Am. Chem. Soc. 143 (2021) 13887–13894.
[13] K. Wu, D. Liu, L. Zhu, T. Wu, Y. Xu, C. He, Y. Xiong, Z. Zhao, B.Z. Tang, Commun. Chem. 8 (2025) 85.
[14] H. Bhatia, D. Ray, J. Phys. Chem. C 123 (2019) 22104–22113.
[15] H. Bhatia, I. Bhattacharjee, D. Ray, J. Phys. Chem. Lett. 9 (2018) 3808–3813.
[16] N. Acharya, S. Dey, R. Deka, D. Ray, ACS Omega 7 (2022) 3722–3730.
[17] H. Bhatia, S. Dey, D. Ray, ACS Omega 6 (2021) 3858–3865.
[18] X. Jin, S. Wang, J. Bian, F. Peng, M.F. Li, Adv. Funct. Mater. (2025) e16635.
[19] J. Yang, X. Zhen, B. Wang, X. Gao, Z. Ren, J. Wang, Y. Xie, J. Li, Q. Peng, K. Pu, Nat. Commun. 9 (2018) 840.
[20] M. Fang, J. Yang, Z. Li, Prog. Mater. Sci. 125 (2022) 100914.
[21] J. Yang, M. Fang, Z. Li, Acc. Mater. Res. 2 (2021) 644–654.
[22] N.J. Turro, V. Ramamurthy, J.C. Scaiano, Principles of Molecular Photochemistry: an Introduction, University science books, 2009.
[23] S. Karmakar, S. Dey, M. Upadhyay, D. Ray, ACS Omega 7 (2022) 16827–16836.
[24] S. Dey, A.K. Pal, M. Upadhyay, A. Datta, D. Ray, J. Phys. Chem. B 127 (2023) 9833–9840.
[25] T. Pope, J. Eng, A. Monkman, T.J. Penfold, J. Chem. Theor. Comput. 20 (2024) 1337–1346.
[26] H. Gong, Y. Song, J. He, P. Wang, Y. Xiang, S. Li, J. Yao, B. Liao, Q. Liao, H. Fu, Angew. Chem. Int. Ed. 63 (2024) e202400089.
[27] S. Karmakar, S. Dey, M. Upadhyay, D. Ray, ACS Omega 7 (2022) 16827–16836.
[28] J. Yang, Y. Zhang, X. Wu, W. Dai, D. Chen, J. Shi, B. Tong, Q. Peng, H. Xie, Z. Cai, Y. Dong, X. Zhang, Nat. Commun. 12 (2021) 4883.
[29] W. Zhao, Z. He, B.Z. Tang, Nat. Rev. Mater. 5 (2020) 869–885.
[30] J. Zhang, E. Sharman, L. Yang, J. Jiang, G. Zhang, J. Phys. Chem. C 122 (2018) 25796–25803.
[31] S. Lower, M. El-Sayed, Chem. Rev. 66 (1966) 199–241.
[32] M. Upadhyay, R. Deka, D. Ray, J. Phys. Chem. Lett. 15 (2024) 3191–3196.
[33] I. Bhattacharjee, N. Acharya, H. Bhatia, D. Ray, J. Phys. Chem. Lett. 9 (2018) 2733–2738.
[34] N. Acharya, M. Upadhyay, S. Dey, D. Ray, J. Phys. Chem. C 127 (2023) 7536–7545.
[35] N. Acharya, M. Hasan, S. Dey, S.-C. Lo, E.B. Namdas, D. Ray, Adv. Photonics Res. 2 (2021) 2000201.
[36] S. Karmakar, R. Deka, S. Dey, D. Ray, J. Lumin. 263 (2023) 120029.
[37] Y. Zhu, C. Qu, J. Ye, Y. Xu, Z. Zhang, Y. Wang, ACS Appl. Mater. Interfaces 14 (2022) 47971–47980.
[38] T. Wang, Z. Hu, X. Nie, L. Huang, M. Hui, X. Sun, G. Zhang, Nat. Commun. 12 (2021) 1364.
[39] H. Bhatia, D. Ray, Mater. Adv. 1 (2020) 1858–1865.
[40] L. Huang, B. Chen, X. Zhang, C.O. Trindle, F. Liao, Y. Wang, H. Miao, Y. Luo, G. Zhang, Angew. Chem., Int. Ed. 57 (2018) 16046–16050.
[41] H. Guo, M. Cao, R. Liu, B. Tian, S. Liu, J. Li, S. Li, B. Strehmel, T.D. James, Z. Chen, Nat. Commun. 15 (2024) 1590.
[42] N. Gan, X. Zou, Z. Qian, A. Lv, L. Wang, H. Ma, H.-J. Qian, L. Gu, Z. An, W. Huang, Nat. Commun. 15 (2024) 4113.
[43] B. Xu, Z. Wang, J. Shen, J. Li, Y. Jia, T. Jiang, Z. Gao, X. Wang, X. Meng, J. Phys. Chem. C 126 (2022) 11701–11708.

[44] T. Wang, Z. Hu, X. Nie, L. Huang, M. Hui, X. Sun, G. Zhang, Nat. Commun. 12 (2021) 1364.
[45] Z. He, W. Zhao, J.W. Lam, Q. Peng, H. Ma, G. Liang, Z. Shuai, B.Z. Tang, Nat. Commun. 8 (2017) 416.
[46] T. Itoh, R. Hashimoto, J. Lumin. 132 (2012) 236–239.
[47] T. Itoh, Chem. Rev. 112 (2012) 4541–4568.
[48] J. Li, X. Li, G. Wang, X. Wang, M. Wu, J. Liu, K. Zhang, Nat. Commun. 14 (2023) 1987.
[49] L. Paul, T. Moitra, K. Ruud, S. Chakrabarti, J. Phys. Chem. Lett. 10 (2019) 369–374.
[50] L. Paul, S. Chakrabarti, K. Ruud, J. Phys. Chem. Lett. 8 (2017) 4893–4897.
[51] D.L. Dexter, J. Chem. Phys. 21 (1953) 836–850.
[52] F. Li, A.J. Gillett, Q. Gu, J. Ding, Z. Chen, T.J. Hele, W.K. Myers, R.H. Friend, E. W. Evans, Nat. Commun. 13 (2022) 2744.
[53] X. Luo, Y. Han, Z. Chen, Y. Li, G. Liang, X. Liu, T. Ding, C. Nie, M. Wang, F. N. Castellano, Nat. Commun. 11 (2020) 28.
[54] W. Zhao, T.S. Cheung, N. Jiang, W. Huang, J.W. Lam, X. Zhang, Z. He, B.Z. Tang, Nat. Commun. 10 (2019) 1595.
[55] Z. Li, Y. Han, F. Wang, Nat. Commun. 10 (2019) 3735.
[56] T. Mirkovic, E.E. Ostroumov, J.M. Anna, R. Van Grondelle, G.D. Scholes, Chem. Rev. 117 (2017) 249–293.
[57] J. Jortner, S.-i. Choi, J.L. Katz, S.A. Rice, Phys. Rev. Lett. 11 (1963) 323.
[58] S. Dey, R. Deka, M. Upadhyay, S. Peethambaran, D. Ray, J. Phys. Chem. Lett. 15 (2024) 3135–3141.
[59] N. Acharya, M. Upadhyay, R. Deka, D. Ray, J. Phys. Chem. C 128 (2024) 8750–8758.
[60] S. Dey, M. Hasan, A. Shukla, N. Acharya, M. Upadhyay, S.-C. Lo, E.B. Namdas, D. Ray, J. Phys. Chem. C 126 (2022) 5649–5657.
[61] S. Bruker, S. Saint, Madison, Wisconsin, USA (2002).
[62] G.M. Sheldrick, Acta Crystallogr. C Struct. Chem. 71 (2015) 3–8.
[63] L.J. Farrugia, J. Appl. Crystallogr. 30 (1997), 565-565.
[64] Y.J. Franzke, C. Holzer, J.H. Andersen, T. Begušić, F. Bruder, S. Coriani, F. Della Sala, E. Fabiano, D.A. Fedotov, S. Fürst, J. Chem. theory Comput. 19 (2023) 6859–6890.
[65] F. Weigend, R. Ahlrichs, Phys. Chem. Chem. Phys. 7 (2005) 3297–3305.
[66] F. Weigend, M. Häser, H. Patzelt, R. Ahlrichs, Chem. Phys. Lett. 294 (1998) 143–152.
[67] J. Schirmer, Phys. Rev. A 26 (1982) 2395.